STATUS OF THE MAJORANA DEMONSTRATOR

S. Vasilyev [1,*], *N. Abgrall* [2], *I. J. Arnquist* [3],
F. T. Avignone III [4,5], *C. X. Balderrot-Barrera* [5], *A. S. Barabash* [6],
F. E. Bertrand [5], *A. W. Bradley* [2], *V. Brudanin* [1], *M. Busch* [7,8],
M. Buuck [9], *D. Byram* [10], *A. S. Caldwell* [11], *Y.-D. Chan* [2],
C. D. Christofferson [11], *C. Cuesta* [9], *J. A. Detwiler* [9],
Yu. Efremenko [12], *H. Ejiri* [13], *S. R. Elliott* [14], *A. Galindo-Uribarri* [5],
T. Gilliss [8,15], *G. K. Giovanetti* [8,15], *J. Goett* [14], *M. P. Green* [5],
J. Gruszko [9], *I. Guinn* [9], *V. E. Guiseppe* [4], *R. Henning* [8,15],
E. W. Hoppe [3], *S. Howard* [11], *M. A. Howe* [8,15], *B. R. Jasinski* [10],
K. E. Keeter [16], *M. F. Kidd* [17], *S. I. Konovalov* [6], *R. T. Kouzes* [3],
B. D. LaFerriere [3], *J. Leon* [9], *J. MacMullin* [8,15], *R. D. Martin* [10],
S. J. Meijer [8,15], *S. Mertens* [2], *J. L. Orrell* [3], *C. O'Shaughnessy* [8,15],
A. W. P. Poon [2], *D. C. Radford* [5], *J. Rager* [8,15], *K. Rielage* [14],
R. G. H. Robertson [9], *E. Romero-Romero* [12,5], *B. Shanks* [8,15],
M. Shirchenko [1], *N. Snyder* [10], *A. M. Suriano* [11], *D. Tedeschi* [4],
J. E. Trimble [8,15], *R. L. Varner* [5], *K. Vetter* [2], *K. Vorren* [8,15],
B. R. White [5], *J. F. Wilkerson* [5,8,15], *C. Wiseman* [4], *W. Xu* [14],
E. Yakushev [1], *C.-H. Yu* [5], *V. Yumatov* [6], *I. Zhitnikov* [1]
(The Majorana Collaboration)

[1] Joint Institute for Nuclear Research, Dubna

[2] Nuclear Science Division, Lawrence Berkeley National Laboratory, Berkeley, CA, USA

[3] Pacific Northwest National Laboratory, Richland, WA, USA

[4] Department of Physics and Astronomy, University of South Carolina, Columbia, SC, USA

[5] Oak Ridge National Laboratory, Oak Ridge, TN, USA

[6] Institute for Theoretical and Experimental Physics, Moscow

[7] Department of Physics, Duke University, Durham, NC, USA

[8] Triangle Universities Nuclear Laboratory, Durham, NC, USA

[9] Center for Experimental Nuclear Physics and Astrophysics and Department of Physics,
University of Washington, Seattle, WA, USA

*E-mail: svasilyev@jinr.ru

[10] Department of Physics, University of South Dakota, Vermillion, SD, USA

[11] South Dakota School of Mines and Technology, Rapid City, SD, USA

[12] Department of Physics and Astronomy, University of Tennessee, Knoxville, TN, USA

[13] Research Center for Nuclear Physics and Department of Physics,
Osaka University, Ibaraki, Osaka, Japan

[14] Los Alamos National Laboratory, Los Alamos, NM, USA

[15] Department of Physics and Astronomy, University of North Carolina,
Chapel Hill, NC, USA

[16] Department of Physics, Black Hills State University, Spearfish, SD, USA

[17] Tennessee Tech University, Cookeville, TN, USA

The Majorana Collaboration is constructing the Majorana Demonstrator, an ultra-low background, 40-kg modular high purity Ge (HPGe) detector array to search for neutrinoless double-beta decay ($0\nu\beta\beta$ decay) in ^{76}Ge. The goal of the experiment is to demonstrate a background rate at or below 3 counts/(t·y) in the 4 keV region of interest (ROI) around the 2039 keV Q-value for ^{76}Ge $0\nu\beta\beta$ decay. In this paper, the status of the Majorana Demonstrator, including its design and measurements of properties of the HPGe crystals, is presented.

PACS: 14.60.Pq; 23.40.-s; 29.40.-n

INTRODUCTION

Neutrinoless double-beta decay searches represent the only viable experimental method to determine the Dirac–Majorana nature of the neutrino [1, 2]. The observation of this process would immediately imply that lepton number is violated. Furthermore, the Majorana nature of the neutrino would allow for the see-saw mechanism [3, 4] to explain the, seemingly finely tuned, small neutrino masses. Finally, the rate of $0\nu\beta\beta$ decay could be used to determine the neutrino mass scale [5]. The $0\nu\beta\beta$-decay rate may be written as:

$$(T_{1/2}^{0\nu})^{-1} = G^{0\nu}|M_{0\nu}|^2 \left(\frac{\langle m_{\beta\beta}\rangle}{m_e}\right)^2, \tag{1}$$

where $G^{0\nu}$ is a phase space factor including the couplings, $M_{0\nu}$ is a nuclear matrix element, m_e is the electron mass, and $m_{\beta\beta}$ is the effective Majorana neutrino mass. The latter is given by

$$\langle m_{\beta\beta}\rangle = \left|\sum_{i=0}^{3} U_{ei}^2 m_i\right|, \tag{2}$$

where U_{ei}^2 specifies the admixture of neutrino mass eigenstate i in the electron neutrino. Then, assuming that $0\nu\beta\beta$ decay is mainly driven by the exchange

of light Majorana neutrinos, it is possible to establish an absolute scale for the neutrino mass, provided that nuclear matrix elements are known.

Experimentally, $0\nu\beta\beta$ decay can be detected by searching the spectrum of the summed energy of the emitted electrons for a monoenergetic line at the Q-value of the decay ($Q_{\beta\beta}$). In previous-generation searches, the most sensitive limits on $0\nu\beta\beta$ decay came from the Heidelberg–Moscow experiment [6] and the IGEX experiment [7], both using ^{76}Ge. A direct observation of $0\nu\beta\beta$ decay was claimed by a subgroup of the Heidelberg–Moscow collaboration [8]. Recent sensitive searches for $0\nu\beta\beta$ have been carried out in ^{76}Ge (GERDA [9]) and ^{136}Xe (KamLAND-Zen [10] and EXO-200 [11]), setting limits that do not support such a claim.

The sensitivity of a $0\nu\beta\beta$ search increases with the exposure of the experiment, but ultimately depends on the achieved background level. This relationship is illustrated in Fig. 1, where the 3σ discovery level for the ^{76}Ge $0\nu\beta\beta$-decay half-life as a function of exposure in tonne-years for 4 different background levels is shown. The horizontal lines indicate the required half-life to reach the bottom of the inverted-hierarchy region (15 meV) for 4 different matrix element calculations and $g_A = 1.27$. The detection efficiency is taken to be 75%.

In order to reach the neutrino mass scale associated with the inverted mass hierarchy, 15–50 meV, a half-life sensitivity greater than 10^{27} y is required. This corresponds to a signal of a few counts or less per tonne-year in the $0\nu\beta\beta$ peak. Observation of such a small signal will require tonne-scale detectors with background contributions at or below a rate of 1 count/(ROI $\cdot$ t $\cdot$ y).
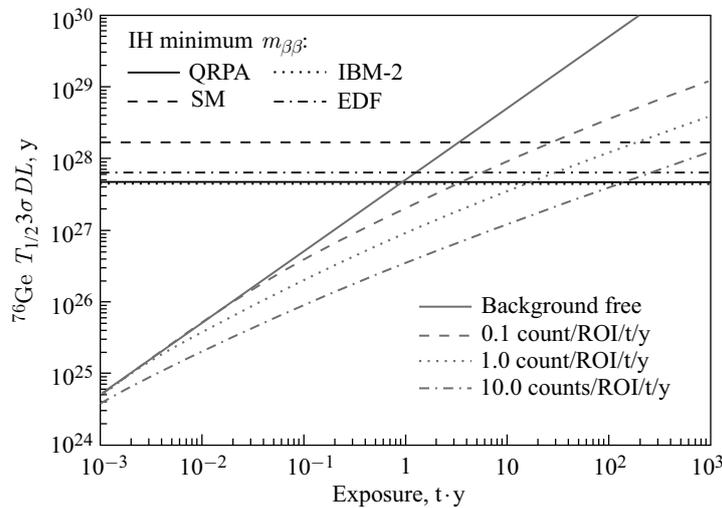
Fig. 1. The 3σ discovery level for the ^{76}Ge $0\nu\beta\beta$-decay half-life as a function of exposure under different background scenarios

1. THE MAJORANA DEMONSTRATOR: OVERVIEW

The Majorana Demonstrator (MJD) [12] is an array of enriched and natural germanium detectors that will search for the $0\nu\beta\beta$ decay of ^{76}Ge. The specific goals of the MJD are:

• Demonstrate a path forward to achieving a background rate at or below 1 count/(ROI·t·y) in the 4 keV region of interest around the 2039 keV $Q_{\beta\beta}$ of the ^{76}Ge $0\nu\beta\beta$ decay.

• Show technical and engineering scalability toward a tonne-scale instrument.

• Perform searches for other physics beyond the Standard Model, such as dark matter and axions.

To this end, the Collaboration is building the Demonstrator, a modular instrument composed of two cryostats built from ultra-pure electroformed copper, each can house over 20 kg of HPGe detectors contained in an ultra-low background structure that maximizes the concentration of crystals while minimizing the amounts of structural materials. Cryostats are mounted on moveable transporters allowing independent assembly and testing before installation into the shield. The array will contain 29 kg of detectors fabricated from 87% enriched ^{76}Ge and 15 kg of detectors from natural Ge (7.8% ^{76}Ge).

Starting from the innermost cavity, the cryostats will be surrounded by an inner layer of electroformed copper (5 cm), an outer layer of Oxygen-Free High thermal Conductivity (OFHC) copper (5 cm), high-purity lead (45 cm), an active muon veto (nearly 4π), borated polyethylene (5 cm), and polyethylene (25 cm) (see Fig. 2). The cryostats, copper, and lead shielding will all be enclosed in a radon exclusion box. The Rn enclosure is a gas tight barrier whose internal volume will be continuously purged with liquid nitrogen boil-off gas to reduce Rn levels near the cryostats. Inside the polyethylene shield two layers of active
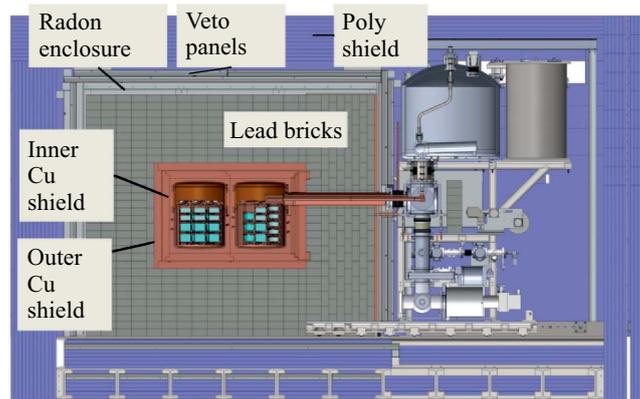
Fig. 2. Cross-sectional view of the Majorana Demonstrator

veto panels on all six sides of the apparatus will be installed. Veto panels are made out of 2.54 cm thick plastic scintillator and are read out by photo-multiplier tubes (PMTs). Detailed design of the veto panels is described in [13]. The entire experiment will be located in a clean room at the 4850 feet level of the Sanford Underground Research Facility (SURF) in Lead, South Dakota, USA [14].

An essential aspect of the Demonstrator is the production and use of ultra-clean Cu. In typical materials uranium and thorium decay-chain contaminants are found at levels of μg/g to ng/g, which would produce unacceptable background in the Demonstrator. Electroforming copper in a carefully controlled and clean environment allows one to produce copper with U and Th below the level of 10^{-12} g/g [15]. The copper being produced by the Majorana Collaboration has about ten times lower U and Th impurities than commercial electroformed copper, with a projected level of $7.4 \cdot 10^{-14}$ g/g for Th or lower. To avoid cosmogenic activation of the most sensitive parts, the copper is being produced at an underground (UG) production facility at SURF and at a shallow facility at Pacific Northwest National Laboratory, and is being machined UG in an ultra-clean machine shop installed and operated by the Collaboration. Copper has mechanical, thermal, and electrical properties that are suitable for the Demonstrator's cryostats, detector mounts, and inner shield.

The Majorana Collaboration choose to use a modular approach to construct the experimental apparatus. Four or five individual HPGe detectors and their
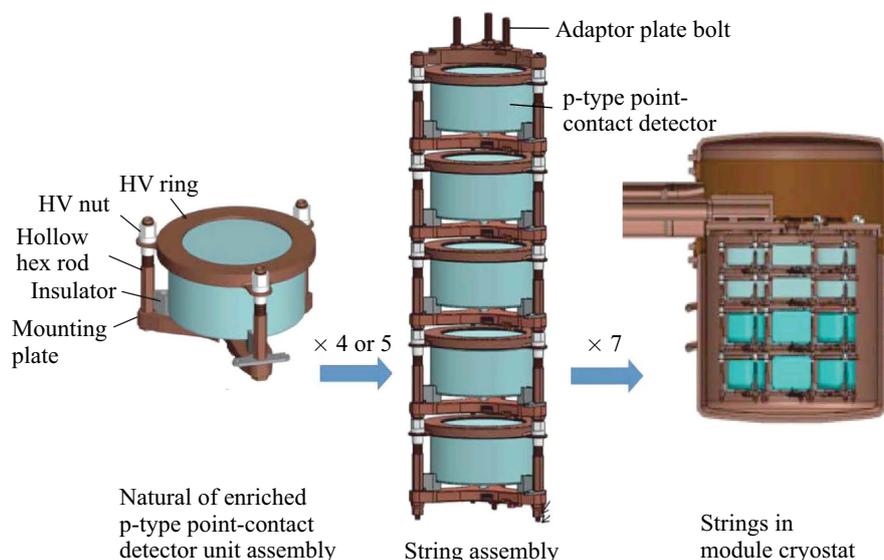
Fig. 3. The modular approach of Majorana Demonstrator. Each module hosts seven strings with four or five detectors

associated low-mass low-radioactivity mounting structures and electronics are stacked together into one string assembly, and seven string assemblies are installed into one cryostat, as shown in Fig. 3.

2. STATUS OF THE MAJORANA DEMONSTRATOR

The construction of the Demonstrator is organized in three phases. In the first phase, a prototype cryostat made of commercial OFHC copper with three strings of natural HPGe detectors was constructed in 2013 and is taking data. The goal of this prototype is to demonstrate the integration of the various components (detectors, vacuum, cooling, shielding, data acquisition). Most of the natural Ge detectors are the Broad Energy Ge detectors (BEGe) manufactured by Canberra [16], and two natural Ge detectors are manufactured by AMETEK/ORTEC® [17].

Ten natural HPGe detectors of both BEGe and ORTEC® types are arranged into three strings and mounted under the cold plate inside the prototype module cryostat. DAQ systems based on the Object-Oriented Real-time Control and Acquisition (ORCA) platform [18] have been instrumented to control both commercial and collaboration-manufactured electronics. Using this system, background and calibration data are taken. The HPGe detectors in the prototype cryostat have shown good energy resolution similar to that in commercial cryostats. As an example, a spectrum taken by one of the HPGe detectors during a calibration run with a ^{228}Th source is shown in Fig. 4. The Full Width at Half Maximum (FWHM) at 2615 keV is 3.2 keV.

The Demonstrator uses p-type point-contact (PPC) HPGe detectors [19, 20] that have masses in the range of 0.6–1.1 kg. PPC style detectors were chosen after extensive R&D by the Collaboration for their advantages: simple fabrication and very low capacitance, providing a low-energy threshold that allows the reduction of background from cosmogenically produced ^{68}Ge.

These detectors have all the benefits of coaxial HPGe detectors traditionally used for $0\nu\beta\beta$, but also possess superb pulse shape analysis (PSA) discrimination between single-site interactions (such as $0\nu\beta\beta$-decay events) and multi-site interaction events (such as Compton scattering of γ-ray backgrounds), making them highly suitable for $0\nu\beta\beta$ searches.

Measured signals from a PPC detector are shown in Fig. 5. Both charge and current pulses are shown in this figure, for a single-site (*a*) and a multi-site (*b*) γ-ray events. The difference in signal shape is apparent, with four distinct interactions evident in Fig. 5, *b*. The Majorana Collaboration uses two different types of PSA algorithms to discriminate between these two classes of events. The first of these, developed by the GERDA collaboration [21], compares the maximum height of the current pulse (A) to the total energy of the event (E) as determined from the height of the charge pulse. Multiple interactions result in multiple charge pulses separated in time and therefore in a reduced value of A/E.
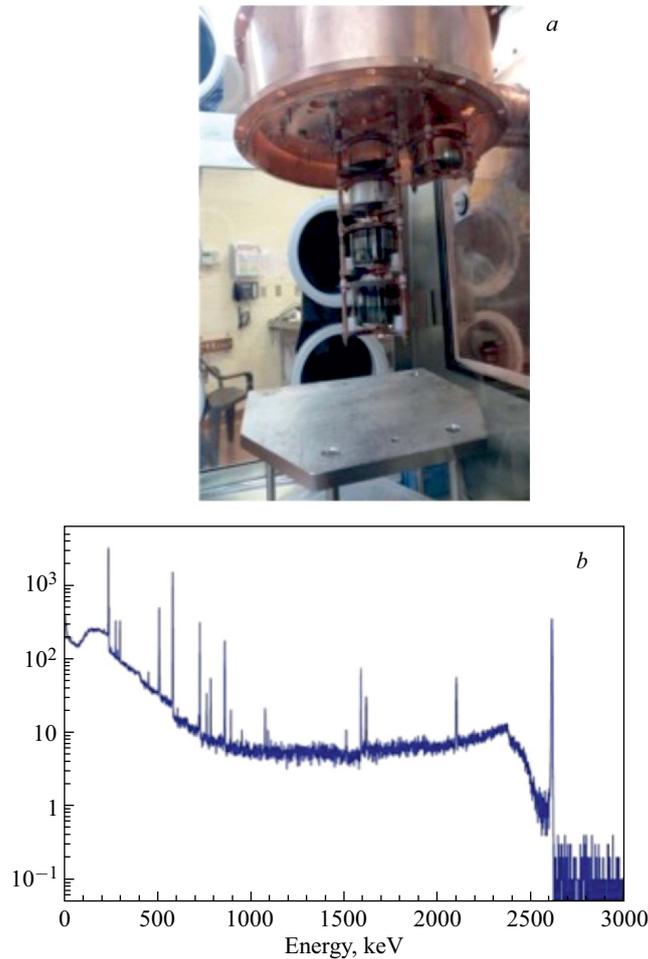
Fig. 4. *a*) A photograph inside the prototype cryostat which is opened up to allow the mounting of three strings of HPGe detectors. *b*) A spectrum taken by one of the HPGe detectors in the prototype cryostat during a calibration run with a ^{228}Th source

As an example, results of this PSA algorithm on PPC data taken by one of the HPGe detectors are shown in Fig. 5, *c*, where the high spectrum is all events from a ^{228}Th source, and the low spectrum is for events that pass the PSA cut. The peak at 1592 keV is the double-escape peak from the pair production interaction of the 2615 keV gamma ray in ^{208}Tl, the final daughter in the Th chain. The double-escape peak has a similar two-β event topology and serves as a proxy for the $0\nu\beta\beta$-decay signal. The algorithm retains at least 90% of these events, while
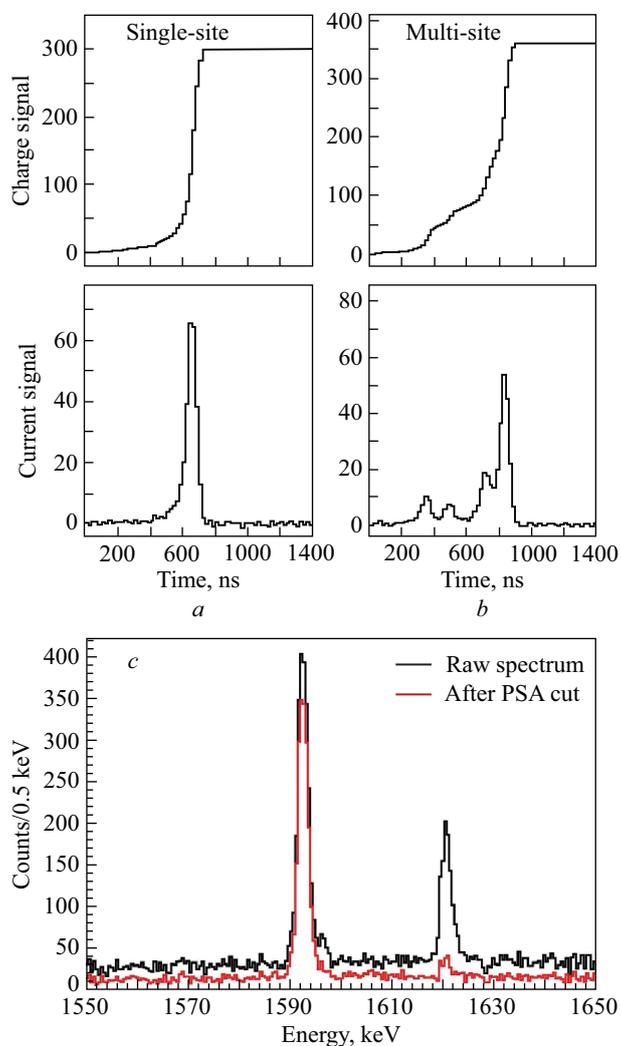
Fig. 5. *a*) Charge and current pulse response of a PPC detector to single-site γ-ray events. *b*) Charge and current pulse response of a PPC detector to multi-site γ-ray events. *c*) Pulse-shape analysis results for PPC data. The high spectrum is for all events within the energy range, while the low spectrum is for events that pass the PSA cut

rejecting up to 90% of the single-escape, multi-site events. The conclusion from these measurements is that pulse shape analysis is a very effective background reduction technique with point-contact Ge detectors.

In the second phase, the first module made from electroformed copper has been populated with a mix of natural and enriched HPGe detectors (see Fig. 6) and will run inside the completed shield. All of the enriched Ge detectors are manufactured by AMETEK/ORTEC[R] [17]. At the moment, first module is under commissioning.

Finally, in the third phase, a second cryostat made of electroformed copper and containing a mix of natural and enriched HPGe detectors will join the first module in the shield. At present, 25.2 kg of enriched germanium detectors are underground and Majorana is aiming for an additional ≈ 4 kg of detectors from the recovery of scrap material. All enriched detectors are extensively tested and characterized in their vendor cryostat both at ORTEC[R] and at SURF. The
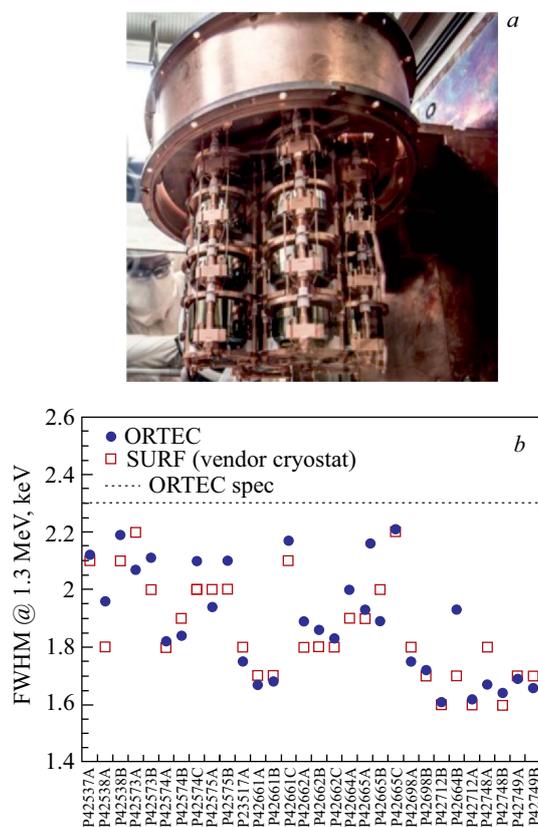
Fig. 6. *a*) A photograph inside the first module made from electroformed copper which is opened up to allow the mounting of seven strings of HPGe detectors. *b*) Energy resolution at 1332.5 keV of the 30 enriched detectors measured by ORTEC[R] (dots) and by MJD collaboration at SURF (open squares), plotted against detector serial number

tests include measurements of the mass, impurity concentration, depletion and operating voltages, leakage current, energy resolution, electronic noise, dead layer, relative efficiency compared to a 3×3-inch NaI(Tl) detector, and pulse-shape discrimination performance.

A number of measurements are performed with various sources placed 25 cm above the top surface of the cryostat. Data taken with ^{60}Co are used to determine the detector energy resolution at 1332.5 keV and the detection efficiency relative to a 3×3-inch NaI(Tl) detector. The FWHM of all detectors are better than the experimental specification of 2.3 keV, which is shown as the dotted horizontal line (see Fig. 6, b).

Prior to the final installation of the strings in the module cryostats, they are again tested in the String Test Cryostat (STC). The goal of these tests is to check the integrity of the detector, front-end electronics and HV connection after the re-installation of the detector in the Majorana mount.

CONCLUSIONS

The Collaboration has developed a number of techniques and materials including electroformed copper to achieve a projected background of < 3.1 counts/(ROI$\cdot$t$\cdot$y). A prototype module with three strings of ^{nat}Ge detectors was constructed in 2013 and has been in running since Summer of 2014. All enriched detectors met requirements during characterization in the vendor cryostat at ORTEC$^{\circledR}$ and SURF. The Majorana Demonstrator is commissioning the first module with 16.8 kg of enriched Ge detectors. Measurements in the STC showed positive results with respect to integrity and performance of the detectors in the Majorana mounts.

REFERENCES

1. *Camilleri L., Lisi E., Wilkerson J. F.* Neutrino Masses and Mixings: Status and Prospects // Ann. Rev. Nucl. Part. Sci. 2008. V. 58. P. 343–369.

2. *Avignone F. T. III, Elliott S. R., Engel J.* Double Beta Decay, Majorana Neutrinos, and Neutrino Mass // Rev. Mod. Phys. 2008. V. 80. P. 481–516.

3. *Gell-Mann M., Ramond P., Slansky R.* Supergravity. Amsterdam: North-Holland, 1979. 315 p.

4. *Mohapatra R. N., Senjanovic G.* Neutrino Mass and Spontaneous Parity Violation // Phys. Rev. Lett. 1980. V. 44. P. 912–915.

5. *Vergados J., Ejiri H., Simkovic F.* Theory of Neutrinoless Double-Beta Decay // Rep. Prog. Phys. 2012. V. 75. P. 106301.

6. *Baudis L. et al. (The Heidelberg–Moscow Experiment).* Limits on the Majorana Neutrino Mass in the 0.1 eV Range // Phys. Rev. Lett. 1999. V. 83. P. 41–44.

7. *Aalseth C. E. et al. (The IGEX Collab.).* IGEX ^{76}Ge Neutrinoless Double-Beta Decay Experiment: Prospects for Next Generation Experiments // Phys. Rev. D. 2002. V. 65. P. 092007.

8. *Klapdor-Kleingrothaus H. V., Krivosheina I. V.* The Evidence for the Observation of 0Nu Beta Beta Decay: The Identification of 0Nu Beta Beta Events from the Full Spectra // Mod. Phys. Lett. A. 2006. V. 21. P. 1547–1566.

9. *Agostini M. et al. (The GERDA Collab.).* Results on Neutrinoless Double-β Decay of ^{76}Ge from Phase I of the GERDA Experiment // Phys. Rev. Lett. 2013. V. 111. P. 122503.

10. *Gando A. et al. (The KamLAND-Zen Experiment).* Limit on Neutrinoless $\beta\beta$ Decay of ^{136}Xe from the First Phase of KamLAND-Zen and Comparison with the Positive Claim in ^{76}Ge // Phys. Rev. Lett. 2013. V. 110. P. 062502.

11. *Albert J. B. et al. (The EXO Collab.).* Improved Measurement of the $2\nu\beta\beta$ Half-Life of ^{136}Xe with the EXO-200 Detector // Phys. Rev. C. 2014. V. 89. P. 015502.

12. *Abgrall N. et al. (The Majorana Collab.).* The Majorana Demonstrator Neutrinoless Double-Beta Decay Experiment // Adv. High Energy Phys. 2014. V. 2014. P. 365432.

13. *Bugg W., Efremenko Yu., Vasilyev S.* Large Plastic Scintillator Panels with WLS Fiber Readout: Optimization of Components // Nucl. Instr. Meth. A. 2014. V. 758. P. 91–96.

14. *Heise J.* The Sanford Underground Research Facility at Homestake. arXiv:1503.01112v2 [physics-ins.det].

15. *Hoppe E. W. et al.* Microscopic Evaluation of Contaminants in Ultra-High Purity Copper // J. Radioanal. Nucl. Chem. 2009. V. 282. P. 315–320.

16. Meriden, Connecticut, USA: Canberra Industries, 2009.

17. Oak Ridge, Tennessee, USA: ORTEC, 2009.

18. *Howe M. A. et al.* Sudbury Neutrino Observatory Neutral Current Detector Acquisition Software Overview // IEEE Trans. Nucl. Sci. 2004. V. 51. P. 878–883.

19. *Luke P. N. et al.* Low Capacitance Large Volume Shaped-Field Germanium Detector // IEEE Trans. Nucl. Sci. 1989. V. 36. P. 926–930.

20. *Barbeau P. S., Collar J. I., Tench O.* Large-Mass Ultralow Noise Germanium Detectors: Performance and Applications in Neutrino and Astroparticle Physics // JCAP. 2007. V. 2007. 09. P. 9.

21. *Budjas D. et al.* Pulse Shape Discrimination Studies with a Broad Energy Germanium Detector for Signal Identification and Background Suppression in the GERDA Double Beta Decay Experiment // JINST. 2009. V. 4. P. 1–23.